Materials and Design 97 (2016) 131–137

Contents lists available at ScienceDirect

Materials and Design

journal homepage: www.elsevier.com/locate/matdes

Role of volume fraction of second phase particles, dislocation-twin and twin-twin interactions in the reduced tension-compression yield asymmetry

Yan Jiang [a], Yu'an Chen [a,b,*], Gentao Gao [a]

[a] College of Materials Science and Engineering, Chongqing University, Chongqing 400044, China
[b] National Engineering Research Center for Magnesium Alloys, Chongqing University, Chongqing 400044, China

ARTICLE INFO

Article history:
Received 6 January 2016
Received in revised form 18 February 2016
Accepted 19 February 2016
Available online 22 February 2016

Keywords:
{10$\bar{1}$2} twin
Second phase particles
Tension-compression yield asymmetry
Dislocation-twin interaction
Twin-twin interaction

ABSTRACT

In the present study, TZA521 alloy and TZA1021 alloy were designed and subjected to extrusion process as well as extrusion followed by rolling process to uncover the role of volume fraction of second phase particles (Mg_2Sn phase in this work), dislocation-twin and twin-twin interactions in the reduced tension-compression yield asymmetry. Our results show that yield asymmetry is only weakly dependent on the volume fraction of Mg_2Sn phase, owing to the presence of some coarse Mg_2Sn phases and relatively large inter-particle spacing. Grain subdivision by {10$\bar{1}$2} twins and dislocation-twin interactions are found to reduce the tension-compression yield asymmetry of a slip predominant deformation, i.e. tension along the rolling direction in the extrusion followed by rolling condition, while twin-twin interactions mainly account for the reduced tension-compression yield asymmetry during compression along the rolling direction for both alloys in the rolling following extrusion condition. The relevant mechanisms are discussed.

1. Introduction

Magnesium alloys normally develop a strong texture formed during the manufacturing processes (such as rolling and extrusion) and exhibit intensive tension-compression yield asymmetry (expressed as the ratio of the compressive yield stress to the tensile one, CYS/TYS) [1]. For example, for the extruded rods with a fiber texture, intensive yield asymmetry appears during tension and compression along the extrusion direction (ED) [2], where high mechanical asymmetry with a compression to tension ratio between 0.3 and 0.6 is even observed [3]. Strong yield asymmetry along rolling direction (RD), transverse direction (TD), and normal direction (ND) can also be noticed in the hot-rolled plate with a basal texture. Increasing evidences have illustrated that the yield asymmetry is closely related with the {10$\bar{1}$2} twinning [4,5], which constitutes one of the most important deformation mechanisms in Mg alloys owing to the hexagonal close-packed crystal structure. If {10$\bar{1}$2} twinning dominates in compression and slip in tension along the ED of a textured Mg alloy, the stress needed to activate slip is larger than that of {10$\bar{1}$2} twinning. This, in conjunction with the polarity of {10$\bar{1}$2} twinning, gives rise to the tension-compression yield asymmetry [4,5].

Currently, considerable efforts have been made to reduce the yield asymmetry of Mg alloys, among which include hybrid twin structure [6], grain refinement [7], tailoring texture [8,9], and precipitation [10,11]. A hybrid twin structure prepared by a cross compression along TD and RD of the hot-rolled Mg alloy AZ31 re-assigns the crystallographic orientation, thus reducing the yield asymmetry along the RD, TD and ND to a large extent [6]. It has also been demonstrated that precipitate's shape and habit can have a markedly different strengthening effect on different deformation modes [12]. If the deformation modes with a low critical resolved shear stress (CRSS), i.e. basal slip and {10$\bar{1}$2} twinning, can be strengthened more strongly than those which possess a high CRSS (e.g. prismatic slip), then a reduction in asymmetry will be possible. Recently, it is uncovered that the second phase particles ($Mg_{17}Al_{12}$ phase in AZ series) can suppress the propagation of {10$\bar{1}$2} twinning [10], a method having been validated to reduce yield asymmetry. However, studies on the volume fraction of second phase particles on the yield asymmetry are scarce. It has been well established that twin boundaries (TBs) as barriers to dislocation slip result in a high resolved shear stress required to transmit a dislocation across TBs, thereby strengthening alloys [13]. Interactions between twins are often observed in Mg alloys and their interactions have been observed to affect subsequent twin nucleation and growth [14]. Dislocation-twin and twin-twin interactions might exert different effects on hardening slip and twinning and this again holds promise as a method to reduce the yield asymmetry, but to date investigation on this has been rarely

* Corresponding author.
E-mail address: jinliyi22@sina.com (Y. Chen).

http://dx.doi.org/10.1016/j.matdes.2016.02.079
0264-1275/

reported. Strong yield asymmetry in alloys is often detrimental to mechanical properties and results in strange bending characteristics, such as failure initiation on the compression side of bent sheets and tubes. [15]. A quantitative investigation of the effect of volume fraction of second phase particles, and dislocation-twin and twin-twin interactions on the response of yield asymmetry, would advance the basic understanding of the mechanism of yield asymmetry. In the present study, TZA521 alloy and TZA1021 alloy were designed and subjected to extrusion process and extrusion followed by rolling process to uncover the role of volume fraction of second phase particles (Mg_2Sn phase), dislocation-twin and twin-twin interactions in the reduced yield asymmetry. Our results reveal that the volume fraction of Mg_2Sn phase, dislocation-twin and twin-twin interactions play a distinct role in the reduced yield asymmetry. The corresponding mechanisms are studied and discussed.

2. Experiments and methods

2.1. Sample preparation

Alloy ingots with compositions (measured using XRF-800CCDEx-ray fluorescence spectrometer) of Mg-4.92wt%Sn-1.95wt%Zn-0.91wt%Al (TZA521) and Mg-9.31wt%Sn-1.92wt%Zn-0.92wt%Al (TZA1021) were prepared by ZG-0.01 vacuum induction furnace under the protection of argon atmosphere in a steel crucible followed by casting into steel mould. Then, billets ($\Phi = 80$ mm, h = 150 mm) were machined from the cast ingots and subsequently homogenized at 325 °C for 12 h followed by at 440 °C for 10 h. The as-homogenized billets were extruded at 330 °C using an extrusion ratio of 25, with an extrusion rate of 0.5 mm s^{-1}. Some extruded samples were also machined into rectangular blocks with dimensions of 70 mm long (extrusion direction, ED), 10 mm wide (radial direction, ERD) and 12 mm thick (tangential direction, ETD), which were subsequently subjected to hot rolling along the ED at 400 °C with total thickness reductions of 67% and about 10% reduction in each pass. Tensile specimens were cut from the extrusion rods along the ED and plates after rolling along the RD, and then machined into dog bone shape of 10 mm in gauge length and 4 × 2.5 mm in cross section. Compressive specimens (6 mm in height × 4 mm in width × 4 mm in length) were prepared for the subsequent compression tests along the same direction. The mechanical tests were performed at room temperature on a Shimadzu AG-X (50 kN) machine using a strain rate of 10^{-3} s^{-1}. An extensometer with a 4 mm gauge length was directly attached to the tensile samples for strain measurement. Each test was repeated three times.

2.2. Microstructure and texture analysis

For the examination of microstructure by optical microscopy and scanning electron microscopy (SEM; TESCAN VEGAII scanning electron microscope equipped with an Oxford Instruments INCA Energy 350 energy dispersive X-ray spectrometer (EDS)), the specimens were carefully ground with a series of SiC papers and chemically etched in an acetic picral solution (2 ml acetic acid + 1 g picric acid + 2 ml H_2O + 16 ml ethanol). Pole figures of samples tested at the plane perpendicular to the ED or along the rolling plane were measured using an X-ray diffraction (XRD) analysis (Rigaku D/max-2500PC). Electron back-scattered diffraction (EBSD) mapping was conducted on a scanning electron microscope (FEI Nova 400 FEG-SEM equipped with an HKL channel 5 system and a charge-coupled deviced (CCD) camera) using a step size of 1 μm. The samples for EBSD mapping were mechanical ground followed by electro-chemical polishing in the AC2 commercial electrolyte (Struers, Denmark).

3. Results

3.1. Microstructure

Fig. 1 depicts the optical micrographs (a–d) and SEM images (e–h) of TZA521 alloy and TZA1021 alloy. As seen from the figure, the as-extruded material had a slightly inhomogeneous grain structure with an average linear intercept grain size of ~15 and 14 μm for TZA521 and TZA1021 alloy, respectively. It can be seen that the grain size of both alloys in the rolling following extrusion process (donated as the extrusion + rolling condition) slightly coarsens compared with that of both alloys in the as-extruded condition (donated as the extrusion condition). It should be noted that a number of twins occur for both alloys in the extrusion + rolling condition. The SEM images of the two alloys in different conditions are shown in Fig. 1e–h, where second phase particles mainly comprising coarse second phases in the form of irregular shape and fine second phases in the form of sphere shape located in both grain boundaries and grain interiors. Those second phase particles are then identified by the compound use of the energy-dispersive X-ray spectrometer (EDS) (not shown here) and the X-ray diffraction (XRD) pattern as shown in Fig. 2, wherein it shows that the dominant second phase particles in both alloys is a kind of Mg_2Sn phase. This is consistent with the conclusion that only Mg_2Sn phase in the form of spherical morphology can be detected in the Mg-9.8Sn-3.0Al-0.5Zn (wt%) alloy [16] and other phase only forms when Zn/Al ratio is more than 3 [17]. It is worth noting that larger size of second phase particles in TZA1021

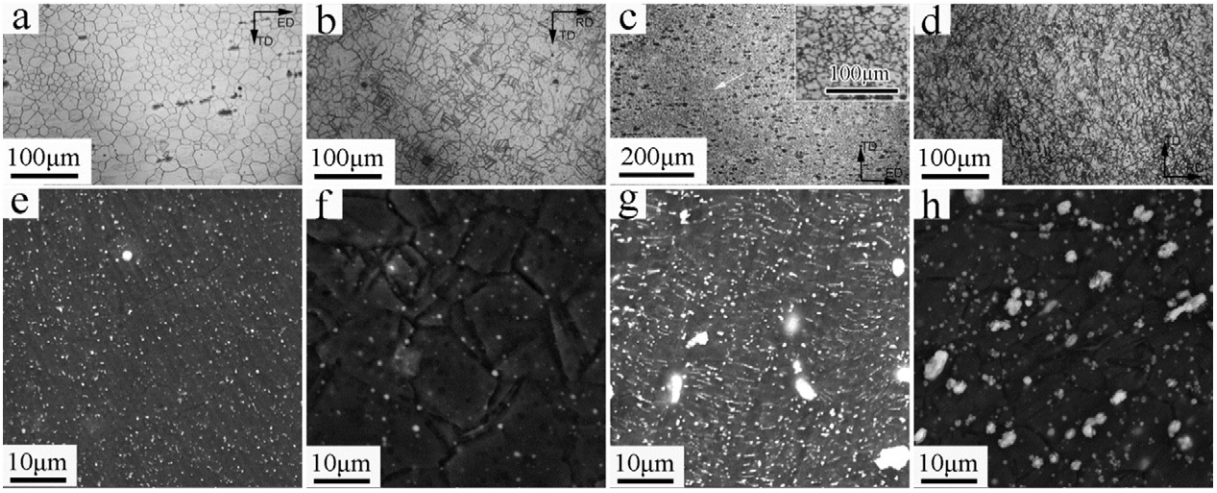

Fig. 1. Optical micrographs (OM) and SEM images of TZA521 alloy: (a) OM and (e) SEM images in the extrusion condition, (b) OM and (f) SEM images in the extrusion + rolling condition, and that of TZA1021 alloy: (c) OM and (g) SEM images in the extrusion condition, (d) OM and (h) SEM images in the extrusion + rolling condition. Note that the white arrow in panel label 'c' indicates the location where the inserted figure with a higher magnification comes from.